Effect of gas mixtures on arc plasma and in-flight $MgAl_2O_4$ particle behavior in plasma spraying

Hunkwan Park[1], Hansol Kwon[1], Yong-jin Kang[1], Yeon Woo Yoo[1], Do Hyun Kim[1], Youngjin Park[1], Sunghun Lee[1] and Changhyuk Kim[2]

[1] *Department of Extreme Environmental Coatings, Korea Institute of Materials Science, Changwon, Korea*
[2] *School of Civil and Environmental Engineering, Pusan National University, Busan, Korea*

Abstract: Plasma spray coating forms a coating by melting powder particles of nano-micro size using the thermal energy of arc plasmas and is particularly widely applied to plasma-resistant coatings of semiconductor parts. In this study, the behavior of $MgAl_2O_4$ powder particles under process conditions such as gas mixtures was investigated using computational analysis to predict the results. The simulation results of the behavior of the powder were verified using DPV eVOLUTION.

Keywords: Thermal spray, thermal plasma modeling, computational simulation, Computational fluid dynamics

1. Introduction

Semiconductor processes, such as etching, sputtering, and chemical vapor deposition, are exposed to fluorocarbon plasma gases, which cause extremely harsh conditions in the equipment. Plasma-resistant materials are frequently coated on the surface of the inner wall of the process chamber or parts for protection. A plasma spray is widely used to produce coatings for plasma resistance because it enables the deposition and modification of coatings. For currently used materials, such as Al_2O_3 and Y_2O_3, the process is well known from previous studies [1, 2]. However, the deposition of alternative materials such as $MgAl_2O_4$ is required, as the semiconductor process undergoes harsher conditions with higher process temperatures and reactive gases. Deposition of $MgAl_2O_4$ with plasma sprays is rarely performed; thus, the correlation between the process parameters and coating characteristics of $MgAl_2O_4$ is not fully understood owing to the complexity of the process with many parameters. The plasma spray process parameters include the arc current, gas mixture powder feeding, and coating distance. Among them, gas mixtures such as argon, hydrogen, nitrogen, and helium significantly influence the deposition of the coating owing to the thermophysical properties of the gases.

In this paper, we present the effect of a gas mixture of argon and hydrogen on a plasma arc and $MgAl_2O_4$ using computational analysis. In addition, the simulation results were validated with an experiment using the powder measurement equipment DPV eVOLUTION.

(1)

2. Mathematical formulation of computational simulation

Figure 1 shows a schematic of the computational model with a 9MB plasma spray gun (Oerlikon Metco). The three-dimensional computational domain includes the plasma torch, powder feeder, and coating distance. Both the arc plasma and interaction between the plasma and particles should be considered in the model. The arc plasma of the plasma torch was predicted using thermal plasma modeling, and the powder particles were investigated using an Eulerian–Lagrangian approach. The local thermodynamic equilibrium (LTE) assumption was applied to the arc plasma [3, 4]. The model solves a set of governing equations, including the equation for mass, momentum, energy, and current continuity. The thermophysical properties of argon and hydrogen to consider the arc plasma were determined using methods by Murphy [5]. The model was developed using a modified OpenFOAM solver to predict the plasma effects.

In addition, the Lagrangian discrete-phase model (DPM) in the software FLUENT was applied to predict the velocity and temperature of a powder particle [6]. The arc plasma was considered to be a continuum, and the in-flight particles were calculated using the Lagrangian approach in FLUENT. The velocity and temperature of the arc plasma at the torch outlet were time-averaged profiles obtained from the arc plasma model.

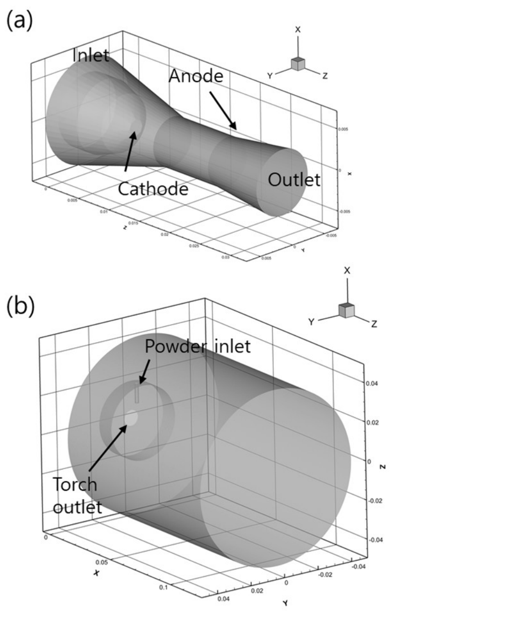

Figure 1. Schematic of (a) plasma torch and (b) powder feeding of the computational model

3. Simulation results

The detailed process parameters are listed in Table 1. The gas mixtures, gas flow rate, and arc current were controlled, and the arc current was calculated using a combination of process conditions. Argon and hydrogen were selected as the process gases. In addition, the carrier gas flow was 13.5 SCFH.

Table 1. Plasma spray process parameters

Process conditions	
Plasma gun	9MB
Ar flow rate (SCFH)	96
H_2, flow rate (SCFH)	0.5, 1, 2, 6, 9, 12, 20
Ac current (A)	600

Fig. 2 shows the predicted temperature and velocity distribution under a 96 Ar/6 H_2 flow rate at 0.01 s. The fluctuation became more intensive with a larger amount of hydrogen because hydrogen has a much larger thermal conductivity and enthalpy than argon, thus resulting in a much faster heat transfer.

A comparison of different conditions was very difficult owing to the intensive fluctuation of the plasma inside the nozzle, as shown in fig. 2. Therefore, the time-averaged distributions of temperature and velocity of the 9MB plasma gun at the outlet were obtained for each gas mixture, as shown in fig. 3. Both temperature and velocity continuously reduced with a larger flow rate of hydrogen because hydrogen can easily disperse owing to its properties. The temperature at the arc fringe decreased because of the faster heat transfer caused by hydrogen. Thus, the larger density of gases at lower temperatures reduced the velocity of the arc plasma. The highest temperature and velocity were observed at a distance of approximately 1 mm from the center of the outlet, which was affected by the intense arc fluctuation. The maximum temperature and velocity of the arc plasma under 96 Ar/0.5 H_2 were 15400 K and 1950 m/s, respectively. The maximum temperature and velocity of the arc plasma under 96 Ar/20 H_2 were 14750 K and 1740 m/s, respectively. The differences in the maximum temperature and velocity were 4% and 10%, respectively. Thus, the addition of hydrogen only slightly affected the temperature and velocity of the arc plasma.

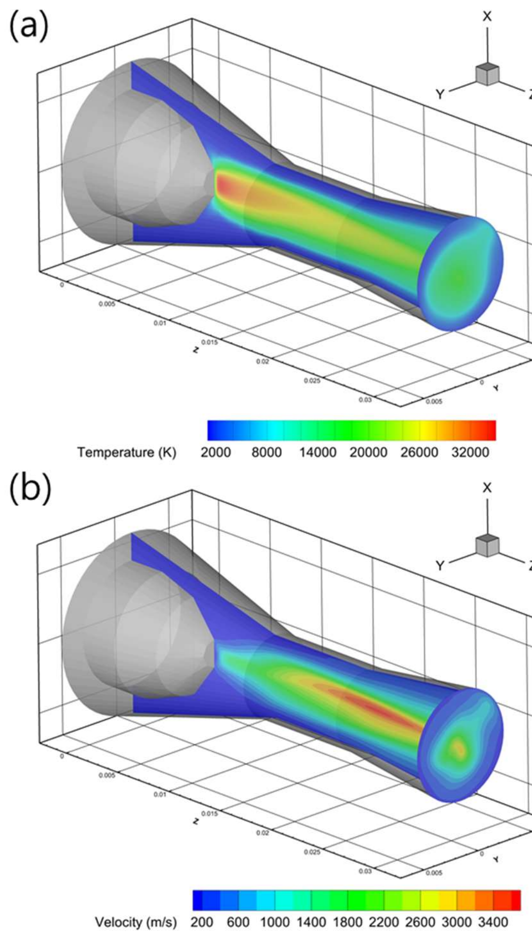

Figure 2. (a) Temperature and (b) velocity distribution of arc plasma for arc plasma under 96 Ar/6 H_2 at 0.01 s

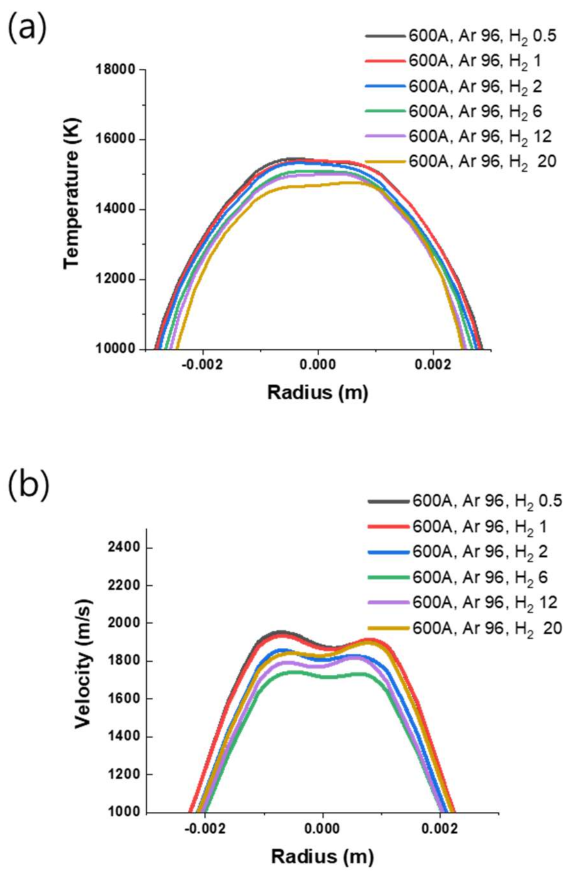

Figure 3. Time-averaged distributions of (a) temperature and (b) velocity of arc plasma at torch outlet

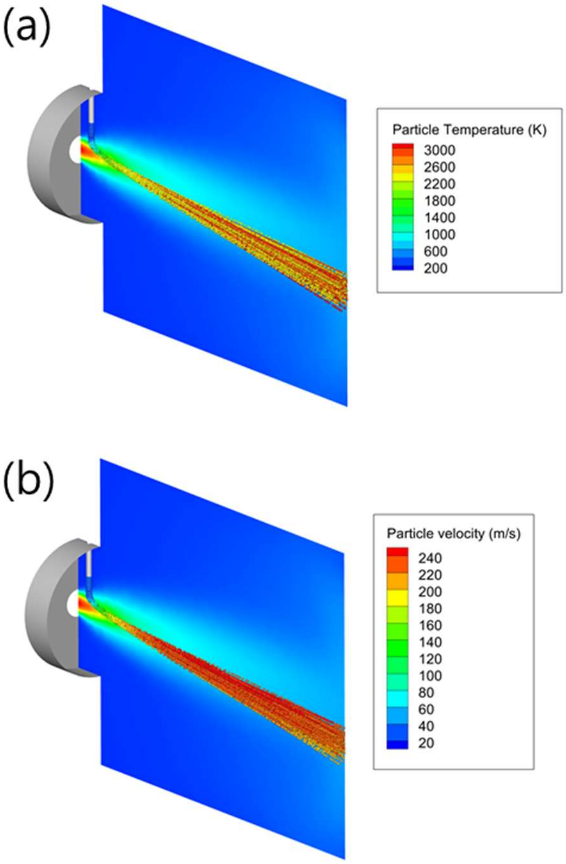

Figure 4. Simulation results of (a) temperature and (b) velocity of in-flight $MgAl_2O_4$ particles under 96 Ar/12 H_2

The effect of the gas mixtures on the inflight of the $MgAl_2O_4$ particles was simulated, as shown in fig. 4. The model of the particle behavior was predicted using the power feeder to the coating distance (100 mm) under six gas mixtures for a diameter of 30 µm. First, $MgAl_2O_4$ particles were injected at room temperature (300 K), and the temperature of the particles dramatically increased owing to heat transfer from the arc plasma. Finally, for 96 Ar/ 12 H_2, the temperature of most of the particles exceeded the melting point of $MgAl_2O_4$ (2408 K). Moreover, the drag force of the plasma flow accelerated the in-flight particles.

4. Comparison with an experiment

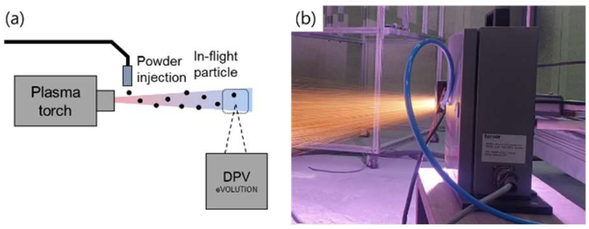

Figure 5. (a)schematic and (b)photograph of the experimental setup for measurement of in-flight particles

For comparison with the experimental measurements, the velocity, temperature, and diameter of the in-flight $MgAl_2O_4$ particles were measured using DPV-eVOLUTION (Tecnar), as shown in fig. 5. A total of 2000 particles were collected and measured at a coating distance (100 mm).

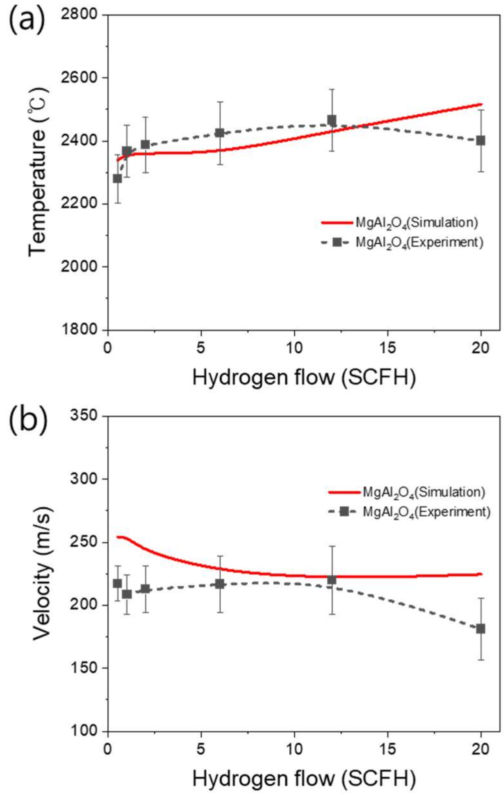

Figure 6. Simulation results of (a)temperature (b)velocity in-flight $MgAl_2O_4$ particles for different gas mixtures

Figure 6 clearly shows a comparison of the temperature and velocity values of the in-flight particles near the coating distance (100 mm) for different gas mixtures. It was very difficult to separate the results of each particle size in the experiment, and the average temperature and velocity for all particles were measured for each condition. In addition, for the simulation, particles of 30 µm were selected, as mentioned previously. The addition of hydrogen slightly decreased the temperature of the arc plasma, as shown in fig. 2. However, the temperature of the in-flight particles increased with a higher hydrogen flow rate, as shown in fig. 6. Therefore, the thermophysical properties of the gas mixture should be considered to determine the process conditions in the plasma spray.

Overall, similar trends were observed in both the simulation and experiment, except for the temperature of 20 H_2. For 20 H_2, the temperature was lower than that of 12 H_2 in the experiment; however, the temperature was higher than that of 12. The simulation result was obtained using the drag force from the arc plasma along with the trajectory, and was the effect of the density and the size of

$MgAl_2O_4$. The density and the size of ceramics such as $MgAl_2O_4$ for the plasma spray are frequently smaller than that of metals to facilitate melting owing to the high melting point of ceramic. Although smaller particles can easily melt, the drag force may not function effectively.

5. Conclusion and future works

In this paper, the initial results of the effect of the gas mixture on the plasma arc and $MgAl_2O_4$ using computational simulations are presented. In addition, the simulation results were validated using experimental measurements. The simulation results demonstrate that the addition of hydrogen is advantageous for the deposition of higher temperatures and velocities of in-flight particles. However, an inflection point was observed, and the optimal condition was not the highest flow rate of hydrogen for $MgAl_2O_4$. Therefore, if the model is improved for in-flight particles with small density and size, this approach can be applied to predict the effect of gas mixtures in plasma sprays.

6. References

[1] J. Kitamura, H. Ibe, F. Yuasa, H. Mizuno, Plasma Sprayed Coatings of High-Purity Ceramics for Semiconductor and Flat-Panel-Display Production Equipment, Journal of Thermal Spray Technology, 17(5-6) (2008) 878-886.

[2] M.I. Boulos, P.L. Fauchais, J.V.R. Heberlein, Thermal Spray Fundamentals, Springer Cham, 2021.

[3] J.P. Trelles, S.M. Modirkhazeni, Variational multiscale method for nonequilibrium plasma flows, Computer Methods in Applied Mechanics and Engineering, 282 (2014) 87-131.

[4] H. Park, M. Trautmann, K. Tanaka, M. Tanaka, A.B. Murphy, A computational model of gas tungsten arc welding of stainless steel: the importance of considering the different metal vapours simultaneously, Journal of Physics D: Applied Physics, 51(39) (2018) 395202-395202.

[5] A.B. Murphy, Transport Coefficients of Hydrogen and Argon–Hydrogen Plasmas, Plasma Chemistry and Plasma Processing, 20(3) (2000) 279-297.

[6] H. Kwon, Y.-j. Kang, Y.W. Yoo, D.H. Kim, Y. Park, S. Lee, H. Park, Effect of Process-Gas Composition on In-Flight and Deposition Characteristics of Atmospheric Plasma-Sprayed Ni Particles, Metals and Materials International, (2022).